Simultaneous Determination of Theophylline and Caffeine Using Poly(L-phenylalanine)-Reduced Graphene Oxide Modified Glassy Carbon Electrode

Lin Zhang[1], Ting Wang[2], Xinxia Fan[1], Dongmei Deng[1,*], Yuanyuan Li[1], Xiaoxia Yan[1], Liqiang Luo[1,*]

[1] College of Sciences, Shanghai University, Shanghai 200444, PR China
[2] School of Health & Social Care, Shanghai Urban Construction Vocational College, Shanghai 201401, PR China
*E-mail: luck@shu.edu.cn (L. Luo); dmdeng@shu.edu.cn (D. Deng)

Theophylline (TP) and caffeine (CF) are two purine alkaloids which widely exist in our human diet. In the present work, poly(L-phenylalanine)-reduced graphene oxide (P(L-Pal)/rGO) modified glassy carbon electrode (GCE) was fabricated and applied to simultaneously determine the concentrations of TP and CF. The P(L-Pal)/rGO composite film was prepared by one-step electropolymerization using cyclic voltammetry, and the surface morphology was investigated by scanning electron microscope. The electrochemical behaviors of TP and CF on P(L-Pal)/rGO/GCE were investigated using cyclic voltammetry and differential pulse voltammetry. By optimizing parameters, the fabricated sensor exhibited excellent performance to simultaneously determine TP and CF in a wide linear range of 1−260 μM. The detection limits were 0.35 and 0.5 μM (S/N = 3), respectively. The presented method shows good sensitivity and stability, and can be used for the determination of TP and CF in samples of green tea, coffee and tablets.

1. INTRODUCTION

Alkaloids are a kind of nitrogen-containing natural organic compounds widely distributed in a variety of plant tissues, most of which contain complex heterocyclic nitrogen structure and possess significant physiological and pharmacological activities [1,2]. Theophylline (TP) and caffeine (CF) are both purine alkaloids existing as the main components in tea, coffee and cocoa drinks. Both TP and CF have multiple pharmacological effects. Theophylline has the effects of strengthening the heart,

diuretic, dilating the coronary arteries, relaxing the bronchial smooth muscle and exciting the central meridian system, so it is mainly used for the treatment of bronchial asthma, emphysema, bronchitis, and cardiac dyspnea [3-8]. Caffeine intake may have some effects on sleep, mood and blood pressure, so it is clinically used as a central nervous stimulant and has analgesic effects [9-12]. However, the tolerance of our human body to the two drugs is limited. When their concentrations in our body are too high, they will cause harm. For example, when the concentration of TP in the blood is too high, it can cause nausea, diarrhea, and arryhythmia, which may result in permanent nerve damage and cardiac arrest [13,14]. Too much caffeine can lead to vascular disease, depression and heart disease, which can bring about cancer and even death [9,15]. Therefore, it is necessary to quickly and accurately determine TP and CF in drugs, beverages or human body.

Since TP and CF are both purine alkaloids, which chemical structures are highly similar, it is difficult to detect them at the same time. So far, many methods have been proposed for the detection of the two drugs, including HPLC [16-18], mass chromatography [19,20], gas chromatography [21], spectroscopic methods [22], capillary electrophoresis [23]. However, most of the above methods require expensive instruments and complex experimental conditions. Electrochemical method can overcome these shortcomings, and it is considered to be the most promising method because of its simple operation and low cost [24-27]. However, due to the similar structures of TP and CF, it is still a challenge to build a new sensor to determine them simultaneously [28]. So far, various sensing materials have been applied to detect TP and CF, including carbon nanomaterials [29-32], noble metal composite materials [33,34], polymer composite materials [35, 36] and so on. Among them, carbon nanomaterials, especially graphene, have been widely used for their excellent electrocatalytic activity [37, 38].

Graphene is a two-dimensional sp^2-hybridized carbon material with single atomic thickness and many attractive properties such as excellent electrical, mechanical, and thermal characteristics [39,40]. Electrochemical sensors based on graphene have also been reported in numerous literatures [41,42]. In particular, graphene oxide (GO), the derivative of graphene, not only retains the layered structure of graphene, but also has abundant oxygen functional hydrophilic groups [43-45]. Since the conductivity of GO is lower than that of graphene, a number of methods have been used to effectively reduce GO into reduced graphene oxide (rGO) to improve conductivity, including microwave and photo catalyst [46], solvothermal [47] chemical [48] and electrochemical reduction methods [49]. Among the methods reported, the preparation of rGO by electrochemical reduction is an ideal method due to its advantages of simplicity, speed, low cost and high efficiency [50]. In addition, rGO prepared by electrochemical reduction has higher conductivity and lower oxygen/carbon ratio than that of chemical reduction method [51].

The polymer modified electrode has proven to be a powerful tool because the thickness, permeability, and charge transfer properties of the film can be adjusted with electrochemical parameters. In addition, the polymer modified electrode possess many benifits of improving electrocatalysis while decreasing surface fouling and undesirable reactions [52]. Actually, electropolymerization have attracted wide attention in the determination of analytes to improve sensitivity, selectivity, uniformity and chemical stability.

Herein, poly(L-phenylalanine)/rGO (P(L-Pal)/rGO) composite film was electropolymerized on glassy carbon electrode (GCE) by cyclic voltammetry (CV) in 0.01 M L-phenylalanine + 0.3 mg.ml^{-1} GO + 0.1 M PBS (pH 2.2) within the potential window of −1.2~2.2 V. The P(L-Pal)/rGO composite showed good catalytic activity for the electrooxidation of TP and CF. The proposed sensor can be applied for the determination of TP and CF in various samples of green tea, coffee and tablets.

2. EXPERIMENTAL

2.1. Chemicals and apparatus

GO, L-phenylalanine, L-asparagic acid, theophylline and caffeine were got from Aladdin Reagents (Shanghai, China). NaCl, Zn(CH$_3$COOH)$_2$·2H$_2$O, MgCl$_2$, Pb(NO$_3$)$_2$, CuCl$_2$·2H$_2$O, glycine, citric acid, sucrose, glutamic acid, glucose, HCl, HNO$_3$, H$_2$SO$_4$ and CH$_3$COOH were purchased from Sinopharm Chemical Reagent Co., Ltd. (China). The chemicals used in the experiments were analytical grade, and Milli-Q water (18.2 MΩ·cm) was applied to prepare all solutions.

CV as well as differential pulse voltammetry (DPV) test was performed on the CHI1030C (Chenhua, China) workstation. The conventional three-electrode system was composed of P(L-Pal)/rGO/GCE as the working, platinum as the counter, and Ag/AgCl as the reference electrodes. The morphology of the synthesized composite film was characterized by scanning electron microscope (SEM, JEOL-6700F, Japan).

2.2. Preparation of modified electrodes

The GCE with diameter of 3 mm was selected as the base material, and a specular smooth GCE surface was obtained by being carefully ground on suede using 1, 0.3 and 0.05 μm Al$_2$O$_3$ powder successively. The polished GCE was then cleaned alternately with ultrapure water and ethanol, followed by 10 consecutive sweeps (CV, −1.0 ~ +1.0 V) in 0.5 M H$_2$SO$_4$ to activate the electrode surface.

Electropolymerization of P(L-Pal)/rGO film was obtained by 6 cyclic scanning from −1.2 to 2.2 V at scanning rate of 80 mV.s^{-1} in 0.01 M L-phenylalanine + 0.3 mg.ml^{-1} GO + 0.1 M phosphate buffer saline (PBS, pH 2.2). Afterwards, the prepared electrode was washed with ultrapure water for further use. For comparison, P(L-Pal) film was prepared with the same process as the above described in 0.01 M L-phenylalanine + 0.1 M PBS (pH 2.2).

3. RESULTS AND DISCUSSION

3.1. Characterization of the P(L-Pal)/rGO composite film

Fig.1a shows CVs of L-phenylalanine polymerizing process in 0.01 M L-phenylalanine + 0.3 mg/ml GO + 0.1 M PBS (pH 2.2) in the potential range of −1.2 ~ 2.2 V. As shown in Fig. 1a, the peak current increased continuously with the increase of cyclic scanning, indicating that the polymer film

grew on the electrode surface continuously. After the modification, uniform blue polymer adhesion film was formed on the electrode surface. From the SEM image Fig. 1b, P(L-Pal)/rGO composite film has been successfully fabricated onto the GCE surface.
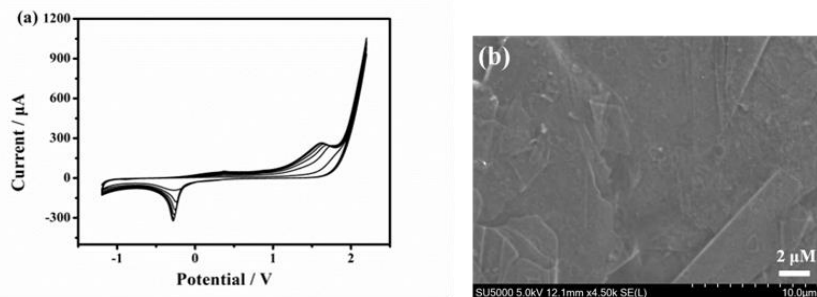

Figure 1. (a) CV of polymerizing process of P(L-Pal)/rGO on GCE surface in 0.1 M PBS (pH 2.2) containing 0.01 M phenylalanine and 0.3 mg.ml^{-1} GO at the scan rate of 80 mV·s^{-1} in the potential range of −1.2 ~ 2.2 V. (b) SEM image of P(L-Pal)/rGO.

3.2. Electrochemical properties of TP and CF

The electrochemical responses of TP and CF at bare GCE, P(L-Pal)/GCE and P(L-Pal)/rGO/GCE were investigated by CV and DPV. Fig. 2a displays CVs of 40 μM TP + 60 μM CF in 0.01 M H$_2$SO$_4$ at different electrodes, respectively. It can be seen from Fig. 2a that, upon the addition of 40 μM TP and 60 μM CF, two irreversible peaks can be observed at 1.24 and 1.40 V, respectively, which should be due to their electrooxidation. Clearly, only poor oxidative current responses were observed on bare GCE. When L-Pal was electropolymerized on the electrode, the peak currents increased significantly, and the current responses of both TP and CF were further enhanced on P(L-Pal)/rGO/GCE. The results in Fig. 2b show that the DPV responses of TP and CF on P(L-Pal)/rGO/GCE were much stronger than those on P(L-Pal)/GCE and bare GCE. These demonstrate that TP and CF exhibited distinguished peak currents with enough separated peak potentials, making it available to determine them simultaneously.
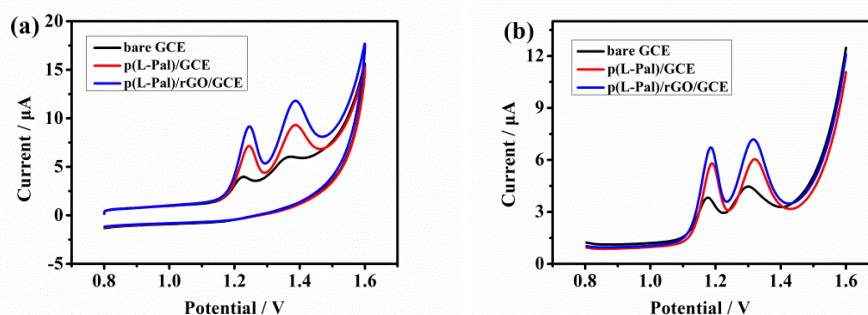

Figure 2. CVs (a) and DPVs (b) of 40 μM TP and 60 μM CF at different kinds of electrodes (Bare GCE, P(L-Pal)/GCE and P(L-Pal)/rGO/GCE) in 0.01 M H$_2$SO$_4$.

The dependences of the oxidation currents of 40 μM TP and 60 μM CF on scan rates were investigated by CV, as illustrated in Fig. 4. From Fig. 4a, the oxidation peak current (I_{pa}) of TP increased linearly with the square root of the scan rate ($v^{1/2}$) in the range of 20−300 mV·s^{-1}. The linear regression equation was found as I_{pa} (μA) = −8.24 + 77.49$v^{1/2}$ (R^2 = 0.998), indicating that the oxidation reaction of TP on P(L-Pal)/rGO/GCE surface is a diffusion-controlled process [53, 54]. At the same time, I_{pa} of CF was directly linear to v in the range from 20−300 mV·s^{-1}. The calibration regression equation was I_{pa} (μA) = 4.65 + 133.19v (R^2 = 0.997), suggesting the oxidation of CF on P(L-Pal)/rGO/GCE is an adsorption-controlled process[55].

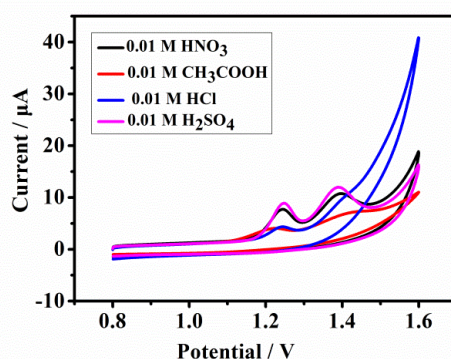**Figure 3.** CVs of 40 μM TP and 60 μM CF at P(L-Pal)/rGO/GCE in different 0.01 M electrolytes: H$_2$SO$_4$, HNO$_3$, CH$_3$COOH and HCl.

3.3. Optimization of the experimental parameters

In order to improve the performance of the sensor, the response of the sensor in different electrolytes was tested by CV. The electrochemical behaviors of 40 μM TP and 60 μM CF were studied on P(L-Pal)/rGO/GCE in different acidic solutions of 0.01 M H$_2$SO$_4$, HNO$_3$, CH$_3$COOH and HCl. By comparing the results in Fig. 3, H$_2$SO$_4$ was chosen as the most suitable electrolyte.
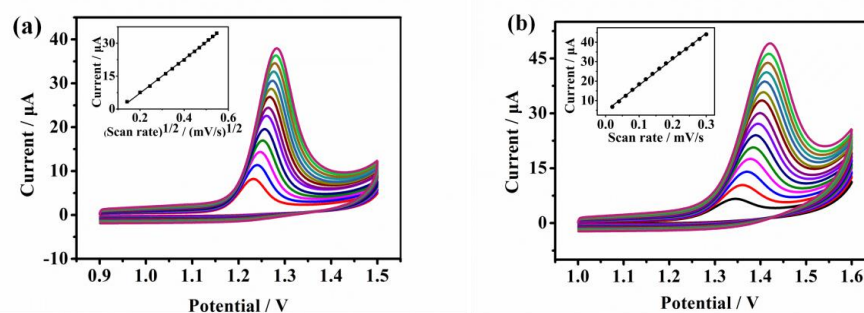

Figure 4. (a) CVs of 40 μM TP in 0.01 M H$_2$SO$_4$ (pH 1.7) at p(L-Pal)/rGO/GCE at different scan rate (20−300 mV·s^{-1}). Inset: the calibration plot of I_{pa} versus square root of scan rate. (b) CVs of 60 μM CF in 0.01 M H$_2$SO$_4$ (pH 1.7) at p(L-Pal)/rGO/GCE at different scan rate (20−300 mV·s^{-1}). Inset: the calibration plot of I_{pa} versus scan rate.

Then, the effect of pH of H_2SO_4 on the changes of oxidation currents at pH 1.3−2.3 was explored by DPV. As shown in Fig. 5a, when pH value increased from 1.3 to 1.7, the oxidation currents increased gradually, and then reached the maximum value at pH 1.7. Afterwards, the peak currents decreased when pH increased further. So, pH 1.7 was chosen (0.01 M H_2SO_4) in the subsequent experiment.

The number of electropolymerization cycles is also an important factor. DPV was used to study the effect of the polymerization cycles of P(L-Pal)/rGO. From Fig. 5b, when the number of electropolymerization cycles was 6, the peak currents reached maximum. When the number of electropolymerization cycles continued to increase, the current decreased, due to the fact that the P(L-Pal) film was too thick. Therefore, 6 cycles were selected for further study.
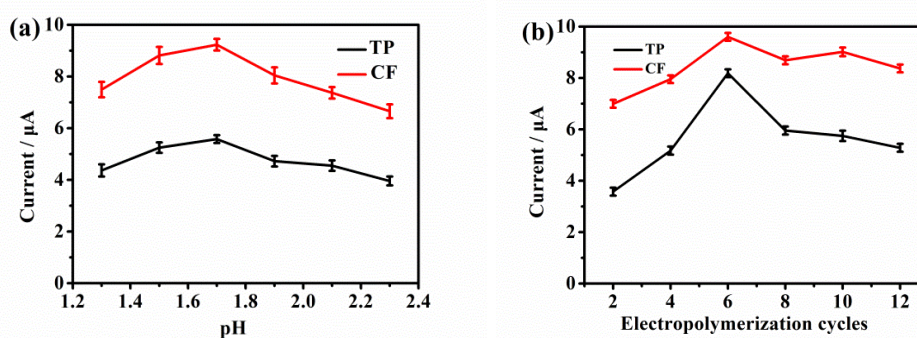

Figure 5. Effects of the pH value (a) and electropolymerization cycles (b) on the oxidation current of 40 µM TP and 60 µM CF at P(L-Pal)/rGO/GCE.

3.4. Quantitative Determination of TP and CF

3.4.1. Individual determination

Under optimal experimental conditions, DPV was applied to the test system by keeping the concentration of one analyte unchanged and gradually changing the concentration of the other one in the solution. As indicated in Fig. 6a, in the presence of 60 µM CF, the peak current was linearly increased with the concentration increasing of TP in the range of 1−300 µM, with the regression equation of I_{pa} (µA) = 1.115 + 0.0865C (µM) (R^2 = 0.997), as displayed in Fig. 6b. Similarly, in 40 µM TP + 0.01 M H_2SO_4, the peak current of CF changed linearly with the concentration of CF in the range of 1−340 µM (Fig. 6c). The linear regression equation between CF concentration and corresponding peak current is: I_{pa} (µA) = 2.35 + 0.057C (µM) (R^2 = 0.998), as shown in Fig. 6d.
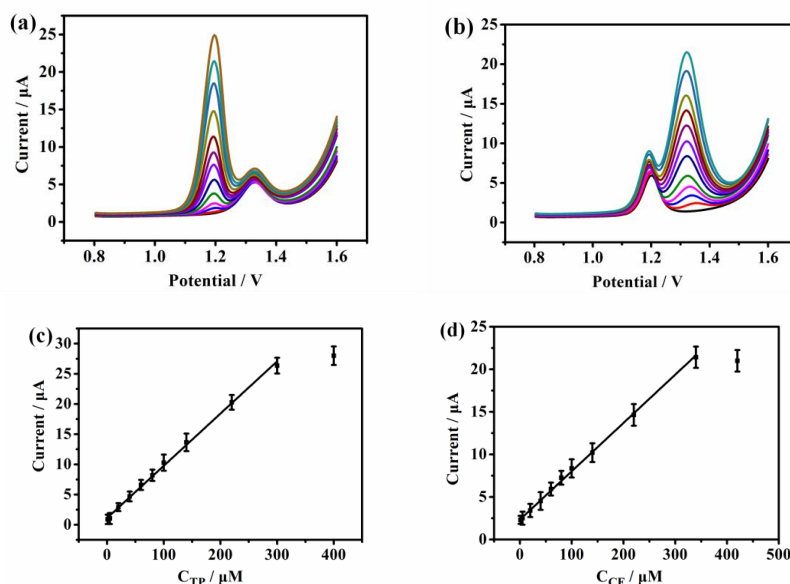
Figure 6. DPVs of determination of TP (1−300 µM) in the presence of 60 µM CF, (b) CF (1−340 µM) in the presence of 40 µM TP onto P(L-Pal)/rGO/GCE in 0.01 M H$_2$SO$_4$ (pH 1.7), (c) and (d):plots of I$_{pa}$ vs. concentrations of TP and CF, respectively.

3.4.2. Simultaneous determination

Simultaneous analysis was also performed with DPV at P(L-Pal)/rGO/GCE in 0.01 M H$_2$SO$_4$ under the optimal experimental conditions established above. DPV curves were recorded by continuously changing TP and CF concentrations simultaneously. As seen from Fig. 7, the peak current increased linearly with their concentrations in the range of 1−260 µM. The regression equations are I$_{pa}$ (µA) = 0.6744 + 0.07992 C$_{TP}$ (µM) (R^2 = 0.997) for TP, and I$_{pa}$ (µA) = 1.174 + 0.059 C$_{CF}$ (µM) (R^2 = 0.997) for CF, respectively. The low detection limits for TP and CF were observed to be 0.35µM and 0.5µM (S/N = 3), respectively. Based on the above results, the proposed P(L-Pal)/rGO/GCE sensor has high sensitivity and excellent linear range, making it a suitable sensor. Table 1 provides a brief comparison of analytical performances on TP and CF at (L-Pal)/rGO/GCE with other modified electrodes in the literature, indicating comparable performance of our proposed sensor [56-59].
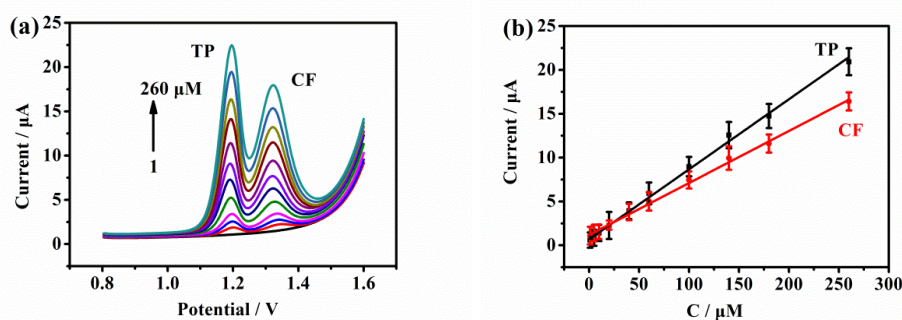

Figure 7. (a) DPVs of simultaneous determination of TP and CF using (L-Pal)/rGO/GCE in 0.01 M H$_2$SO$_4$ (pH 1.7). (b) Calibration plot of the anodic peak currents vs concentration of TP and CF.

Table 1. Comparison of analytical performances of TP and CF at P(L-Pal)/rGO/GCE with other modified electrodes in the literature.

Modified electrode	Analyte	Linear range (μM)	Limit of detection (μM)	Reference
LMC[a]/Nafion/GCE	TP	0.8−180	0.37	[31]
		1.3−230	0.47	
PLCY[b]/N-CNT[c]/GCE	TP	1−70	0.033	[54]
	CF	0.4−140	0.02	
MnO$_2$/IL-Graphene/GCE	TP	1−220	0.1	[56]
Poly(AHNSA)[d]/GCE	CF	10−25	0.79	[57]
P(L-Asp)[e]/f-SWCNTs[f]/GCE	TP	1−50	0.02	[58]
	CF	1−150	0.28	
MWCNT-PE[g]	TP	2−50	0.0197	[59]
P(L-Pal)/rGO/GCE	TP	1−260	0.35	This work
	CF	1−260	0.5	

[a] large mesoporous carbon; [b] poly(L-cysteine); [c] nitrogen-doped carbon nanotubes; [d] poly(4-amino-3-hydroxynaphthalene sulfonic acid); [e] poly(L-aspartic acid); [f] functionalized multi-walled carbon nanotubes; [g] multiwall carbon nanotubes paste electrode.

3.7. Interference studies

To assess the anti-interfering property of the fabricated sensor, some possible interferants were evaluated under the experimental conditions, including inorganic ions of K^+, Na^+, Cu^{2+}, Zn^{2+}, Pb^{2+}, Cl^- and SO_4^{2-} as well as organic molecules of glucose, glycine, citric acid and glutamic acid. During the detection, 1000 μM of possible interfering substances were added in 40 μM TP + 60 μM CF + 0.01 M H_2SO_4. The results show that the addition of interferences did not significantly affect the detection of TP and CF, and thus the proposed sensor possesses good anti-interfering ability.

3.8. Repeatability, reproducibility and stability

P(L-Pal)/rGO/GCE was investigated in 0.01 M H_2SO_4 containing 40 μM TP and 60 μM CF by DPV for test of repeatability, reproducibility and stability. The relative standard deviation (RSD) of current response was 4.3% for five consecutive measurements at the same electrode. On the other hand, the reproducibility was evaluated for three different P(L-Pal)/rGO/GCE, and the RSD of the peak current between them was 2.4%. The results show that the electrode has excellent repeatability and reproducibility. The stability of the sensor was assessed by placing the modified electrode in refrigerator for two weeks and then measuring the current change. The same P(L-Pal)/rGO/GCE kept

93.6% and 92.7% of the initial current values for TP and CF, respectively, demonstrating good stability.

3.9. Real sample analysis

The concentrations of TP and CF in real samples were estimated by standard addition method to appraise the applicability of the fabricated sensor. For such purpose, the contents of TP and CF in different samples of green tea, coffee and theophylline tablet were investigated by DPV, as shown in Table 2. The results show that the presented method can be effectively applied for real samples.

Table 2. Determination of TP and CF in real samples using P(L-Pal)/rGO/GCE.

Sample	Analyte	Determined (µM)	Added (µM)	Found (µM)	Recovery (%)
Green tea	CF	12.6	20.0	33.1	110.5
Coffee	CF	33.5	20.0	52.7	98.5
Tablet	TP	15.4	20.0	36.1	102.0

4. CONCLUSIONS

In this work, P(L-Pal) and rGO were electropolymerized on GCE by CV by 6 cyclic scanning in the potential from −1.2 to 2.2 V at scanning rate of 80 mV.s^{-1} to fabricate P(L-Pal)/rGO/GCE for the simultaneous and sensitive determination of TP and CF. The sensor shows good reproducibility, stability and anti-interference ability. Our work indicates that the proposed P(L-Pal)/rGO/GCE can be effectively applied for the simultaneous determination of TP and CF in different real samples green tea, coffee and tablets.

References

1. A. Mondal, A. Gandhi, C. Fimognari, A.G. Atanasov, A. Bishayee, *Eur. J. Pharmacol.,* 858 (2019) 172472.
2. P.A. Egan, P.C. Stevenson, E.J. Tiedeken, G.A. Wright, F. Boylan, J.C. Stout, *J. Ecol.,* 104 (2016) 1106.
3. T. Igarashi, S. Iwakawa, *Biol. Pharm. Bull.,* 32 (2009) 304.
4. S. Makino, M. Adachi, K. Ohta, N. Kihara, S. Nakajima, S. Nishima, T. Fukuda, T. Miyamoto,

Allergol. Int., 55 (2006) 395.

5. E.E. Ferapontova, E.M. Olsen, K.V. Gothelf, *J. Am. Chem. Soc.,* 130 (2008) 4256.
6. L. Challier, F. Mavré, J. Moreau, C. Fave, B. Schöllhorn, D. Marchal, E. Peyrin, V. Noël, B. Limoges , *Anal. Chem.,* 84 (2012) 5415.
7. T. Gan, J. Li, A. Zhao, J. Xu, D. Zheng, H. Wang, Y. Liu, *Food Chem.,* 268 (2018) 1.
8. S. Tajik, M.A. Taher, H. Beitollahi, *Sens. Actuators, B,* 197 (2014) 228.
9. M.K. McMullen, J.M. Whitehouse, G. Shine, A. Towell, *Food Funct.,* 2 (2011) 197.
10. A. Carolina Torres, M.M. Barsan, C.M.A. Brett, *Food Chem.,* 149 (2014) 215.
11. A. Nehlig, J.L. Daval, G. Debry, *Brain Res. Rev.,* 17 (1992) 139.
12. J.W. Daly, B.B. Fredholm, *Drug Alcohol Depend.,* 51 (1998) 199.
13. E. Molaakbari, A. Mostafavi, H. Beitollahi, *Sens. Actuators, B,* 208 (2015) 195.
14. V. Bellia, S. Battaglia, M.G. Matera, M. Cazzola, *Pulm. Pharmacol. Ther.,* 19 (2006) 311.
15. S. Kerrigan, T. Lindsey, *Forensic Sci. Int.,* 153 (2005) 67.
16. C.W. Huck, W. Guggenbichler, G.K. Bonn, *Anal. Chim. Acta,* 538 (2005) 195.
17. P.D. Tzanavaras, C.K. Zacharis, D.G. Themelis, *Talanta,* 81 (2010) 1494.
18. T. Yoshitake, K. Fujino, J. Kehr, J. Ishida, H. Nohta, M. Yamaguchi, *Anal. Biochem.,* 312 (2003) 125.
19. Y. Yamauchi, A. Nakamura, I. Kohno, M. Kitai, K. Hatanaka, T. Tanimoto, *Chem. Pharm. Bull.,* 56 (2008) 185.
20. Y. Ni, C. Liu, S. Kokot, *Anal. Chim. Acta,* 419 (2000) 185.
21. J.W. Dove, G. Buckton, C. Doherty, *Int. J. Pharm.,* 138 (1996) 199.
22. S. Nafisi, D.S. Shamloo, N. Mohajerani, A. Omidi, *J. Mol. Struct.,* 608 (2002) 1.
23. G. Chen, Q. Chu, L. Zhang, J. Ye, *Anal. Chim. Acta,* 457 (2002) 225.
24. K. Wang, P. Liu, Y. Ye, J. Li, W. Zhao, X. Huang, *Sens. Actuators, B,* 7 (2014) 292.
25. X. Cao, L. Luo, Y. Ding, X. Zou, R. Bian, *Sens. Actuators, B,* 129 (2008) 941.
26. Z. Chu, Y. Liu, Y. Xu, L. Shi, J. Peng, W. Jin, *Electrochim. Acta,* 176 (2015) 162.
27. L. Han, L. Tang, D. Deng, H. He, M. Zhou, L. Luo, *Analyst,* 144 (2019) 685.
28. G. Yang, F. Zhao, B. Zeng, *Talanta,* 127 (2014) 116.
29. Y.H. Zhu, Z.L. Zhang, D.W. Pang, *J. Electroanal. Chem.,* 581 (2005) 303.
30. T. Alizadeh, M.R. Ganjali, M. Zare, P. Norouzi, *Electrochim. Acta,* 55 (2010) 1568.
31. Y. Gao, H. Wang, L. Guo, *J. Electroanal. Chem.,* 706 (2013) 7.
32. V.K. Gupta, A.K. Jain, S.K. Shoora, *Electrochim. Acta,* 93 (2013) 248.
33. G.C. Zhao, X. Yang, *Electrochem. Commun.,* 12 (2010) 300.
34. L. Zi, J. Li, Y. Mao, R. Yang, L. Qu, *Electrochim. Acta,* 78 (2012) 434.
35. S. Guo, Q. Zhu, B. Yang, J. Wang, B. Ye, *Food Chem.,* 129 (2011) 1311.
36. M. Amare, S. Admassie, *Talanta,* 93 (2012) 122.
37. O. Parlak, A. Tiwari, A.P.F. Turner, A. Tiwari, *Biosens. Bioelectron.,* 49 (2013) 53.
38. C. Tan, X. Huang, H. Zhang, *Mater. Today,* 6 (2013) 29.
39. Y. Zhang, Q. Cao, F. Zhu, H. Xu, Y. Zhang, W. Xu, X. Liao, *Int. J. Electrochem. Sci.,* 15 (2020) 8771.
40. A.M.J. Haque, H. Park, D. Sung, S. Jon, S.Y. Choi, K. Kim, *Anal. Chem.,* 84 (2012) 1871.
41. J. Li, D. Kuang, Y. Feng, F. Zhang, Z. Xu, M. Liu, *J. Hazard. Mater.,* 201-202 (2012) 250.
42. P.M. Jahani, S.Z. Mohammadi, A. Khodabakhshzadeh, J.H. Cha, M.S. Asl, M. Shokouhimehr, K. Zhang, L. Quyet Van, W. Peng, *Int. J. Electrochem. Sci.,* 15 (2020) 9037.
43. J. Kim, L.J. Cote, F. Kim, W. Yuan, K.R. Shull, J. Huang, *J. Am. Chem. Soc.,* 132 (2010) 8180.
44. Y. Li, K. Huan, D. Deng, L. Tang, J. Wang, L. Luo, *ACS Appl. Mater. Interfaces,* 12 (2020) 3430.
45. G.P. Kumar, R. Nehru, S.M. Chen, B.M. Almunqedhi, T.W. Chen, J.Y. Wang, M.C. Yu, N.M. Darwish, *Int. J. Electrochem. Sci.,* 14 (2019) 6065.
46. L.J. Cote, R. Cruz-Silva, J. Huang, *J. Am. Chem. Soc.,* 131 (2009) 11027.
47. H. Wang, J.T. Robinson, X. Li, H. Dai, *J. Am. Chem. Soc.,* 131 (2009) 9910.

Int. J. Electrochem. Sci., 16 **(2021)** Article ID: 21041

11

48. M. Zhou, Y. Wang, Y. Zhai, J. Zhai, W. Ren, F. Wang, S. Dong, *Chem. Eur. J.,* 15 (2009) 6116.
49. S.Y. Toh, K.S. Loh, S.K. Kamarudin, W.R.W. Daud, *Chem. Eng. J.,* 251 (2014) 422.
50. H.L. Guo, X.F. Wang, Q.Y. Qian, F.B. Wang, X.H. Xia, *ACS Nano,* 3 (2009) 2653.
51. M.A. Raj, S.A. John, *J. Phys. Chem. C,* 117 (2013) 4326.
52. Y.Z. Zhou, L.J. Zhang, S.L. Chen, S.Y. Dong, X.H. Zheng, *Chin. Chem. Lett.,* 20 (2009) 217-220.
53. Y. Wang, T. Wu, C.Y. Bi, *Microchim. Acta,* 183 (2016) 731-739.
54. Y. Wang, Y. Ding, L. Li, P. Hu, *Talanta,* 178 (2018) 449.
55. J.Y. Sun, K.J. Huang, S.Y. Wei, Z.W. Wu, F.P. Ren, *Colloids Surf., B,* 84 (2011) 421.
56. X. Zhuang, D. Chen, S. Wang, H. Liu, L. Chen, *Sens. Actuators, B,* 251 (2017) 185.
57. M. Tefera, A. Geto, M. Tessema, S. Admassie, *Food Chem.,* 210 (2016) 156.
58. B. Mekassa, M. Tessema, B.S. Chandravanshi, *Sens. Bio-Sens. Res.,* 16 (2017) 46.
59. S.J. Malode, N.P. Shetti, S.T. Nandibewoor, *Colloids Surf., B,* 97 (2012) 1.